Iranian Polymer Journal
20 (12), 2011, 943-954

Available online at: http://journal.ippi.ac.ir

Erosion Rate of Random Short Carbon Fibre/Phenolic Resin Composites: Modelling and Experimental Approach

Masoud Ommati, Iman Fotovat Ahmadi, Seyed Mohammad Davachi, and Siamak Motahari*

School of Chemical Engineering, College of Engineering, University of Tehran, P.O. Box: 11365/4563, Tehran, Iran

Received 18 April 2011; accepted 14 November 2011

ABSTRACT

A model is introduced to describe the erosion rate of random short carbon fibre composites exposed to high speed hot gas flow. A mathematical equation is derived to calculate the erosion rate of the composite using combined solution of the heat conductivity, filtration and kinetic equations of reactions which occur simultaneously in a pyrolysis process. The fibre orientation distribution density function has been employed to determine the mechanical erosion of the composite as well as its chemical erosion and to evaluate the fibres angles with respect to their flow direction. The model describes composite erosion rate as a function of composite surface temperature, hot gas pressure head applied on the material and the thermo-physical properties of the fibres and resin. The DSC and TGA techniques have been employed to measure the ablation kinetic parameters. The thermal conductivity coefficients of the composites have been obtained by Cussons thermal conductivity apparatus. To examine the validity of the results obtained by the model, a series of experiments were carried out using short carbon fibre/phenolic resin composite samples in an oxyacetylene torch. The results obtained from the model are totally in accordance with the experimental data collected from the oxyacetylene flame tests. This model can be effectively used in the design of thermal protection shields, for both material selection and calculation of the materials thickness.

Key Words:

carbon fibre;
phenolic resin;
erosion rate;
mechanical erosion;
thermal degradation.

INTRODUCTION

Ballistic re-entrance of a space vehicle into the earth's atmosphere is subjected to harsh aerodynamic heating. Therefore, its successful return depends mainly on the provisions made for reduction of aerodynamic heat transfer to its structure [1,2]. For hypersonic vehicles subjected to severe aerodynamic heating the integrity of the structure, in the thermal protection systems, is usually maintained by charring the ablative materials.

Ablation is an erosive phenomenon in which the removal of material takes place as a consequence of thermo-mechanical, thermo-chemical, and thermo-physical erosions resulting from high temperature, high pressure and high velocity of the combustion flame. Low thermal conductivity and high thermal stability are critical factors for ablation resistance applications and composite materials have been

(*) To whom correspondence to be addressed.
E-mail: smotahari@ut.ac.ir

proved to meet these requirements. A typical ablation resistance material is often exposed to severe environments and it is obvious that the use of composites can take advantage of their excellent properties (e.g., high chemical stability and high mechanical properties) under these extreme conditions [3]. Carbon-base materials, e.g., carbon-phenolic materials, graphite and three dimensional carbon-carbon structures are very interesting ablative materials as vehicle heat shields for re-entry into earth atmosphere [4]. This interest stems from the resistance of carbon-base materials to ablation, their strength at high temperatures and their ability to maintain extremely high surface temperatures as well as re-radiation of a large amount of energy [5,6].

Short-fibre reinforced composites (SFRC) have been applied in many applications as a class of structural materials due to their relatively low cost, simplicity of fabrication [6-8] and superior mechanical properties [9,10]. Extrusion compounding and injection-moulding techniques are often employed to make short-fibre reinforced composites [11,12]. Short fibres are often misaligned or even damaged due to processing. Hence, in the final composites, there is a kind of fibre orientation distribution (FOD) [13-15].

When a composite is exposed to high temperature and high velocity fluid stream, the decomposition of the resin begins at its pyrolysis temperature and subsequently a char layer is formed at higher temperature. The free surface of the composite under the influence of high temperature stream continuously moves back and it is oxidized depending on the oxygen content of the gases. Therefore, three zones can be distinguished in this process: (i) the virgin material, (ii) the pyrolysis zone and (iii) the porous char layer [1]. In this respect, the ablative composites undergo four main physicochemical processes comprising: chemical reactions (mainly oxidation), sublimation, thermo-mechanical erosion of a composite under the action of an external over-running gas flow, and erosion due to an internal flow of gases generated by thermal decomposition [16].

Ren et al. [4] and Dimitrienko et al. [16] have proposed a number of analytical models to predict the mechanical erosion of the unidirectional or textile composites.

Recently, thermo-mechanical properties and the solid particle erosion performance of short carbon fibre reinforced vinyl ester resin-based composites have been evaluated. It is found that they exhibit superior thermo-mechanical response with highest energy dissipation/damping ability accompanied with a constant storage modulus by modelling the erosion rate with the modulus behaviour by summation method [17]. Vignoles et al. [18] have presented a modelling analysis of the surface evolution of carbon/carbon fibre composites under ablation in the rocket nozzle critical conditions which shows the effect of carbon fibre in the heat shields.

The main objective of this study is to predict the erosion rate of the random short carbon fibre composites. For this reason, the fibre orientation distribution (FOD) method was employed to derive an expression to determine the mechanical erosion of the composite following chemical erosion. The experimental data were also analyzed and compared to the analytical results obtained from the model. A mathematical model was developed to predict the erosion rate of short carbon fibre phenolic composites exposed to a hot gas flow. This model not only considered the thermo-chemical erosion but also the thermo-mechanical erosion of the composite. The main novelties of the current work are the prediction of the composite erosion rate as a function of pressure head and surface temperature with the aid of integral method to modify the results, while all the earlier studies were summation models.

THEORY

Fibre Orientation Distribution (FOD) Method

During extrusion compounding and injection moulding processes, continuous changes in fibre orientation take place in the bulk of moulded components. These changes are intricately related to the size and concentration of the fibres, flow behaviour of the melted polymer matrix, mould cavity, and processing conditions.

A fibre orientation distribution function which represents the inclination angle must have such properties that by variation of its shape parameters being able to describe the changes from a unidirectional distribution to a random distribution

[19]. Fibre orientation can be described by a pair of angles *(θ,ϕ)* as shown in Figure 1. The FOD density function, *g(θ)*, can be defined as follows [19-22]:

$$g(\theta) = \frac{(\sin\theta)^{2r-1}(\cos\theta)^{2q-1}}{\int_{\theta_{min}}^{\theta_{max}} (\sin\theta)^{2r-1}(\cos\theta)^{2q-1}\,d\theta} \quad (1)$$

where *r* and *q* are the shape parameters which can be used to determine the shape of the distribution curve, *r≥1/2* and *q≥1/2*. The angle (*θ*) between the fibre orientation direction and flow of hot gases should be in the range $0 \le \theta_{min} \le \theta \le \theta_{max} \le \pi$. By differentiation of eqn (1) with respect to *θ* and equating the resultant expression to zero the most probable fibre orientation angle (θ_{mod}) is obtained as follows:

$$\theta_{mod} = \arctan\left\{\left[(2r-1)/(2q-1)\right]^{1/2}\right\} \quad (2)$$

When *r* and *q* are set to 1/2, the θ_{mod} cannot be calculated, indicating that the fibres are distributed randomly within the matrix.

Thus, eqn (1) is a suitable probability density function for describing the fibre orientation distribution and it is being used in the present study. The mean fibre orientation, θ_{mean}, can be calculated based on eqn (1) as follows:

$$\theta_{mean} = \int_{\theta_{min}}^{\theta_{max}} \theta g(\theta)\,d\theta \quad (3)$$

g(θ)dθ is the probability density of the fibres with orientation laid in definite intervals. Additionally, the cumulative distribution function of the fibre orientation is given by [21,22]:

$$G(\theta) = \int_{\theta_{min}}^{\theta} g(\theta)\,d\theta = \frac{\int_{\theta_{min}}^{\theta} (\sin\theta)^{2r-1}(\cos\theta)^{2q-1}\,d\theta}{\int_{\theta_{min}}^{\theta_{max}} (\sin\theta)^{2r-1}(\cos\theta)^{2q-1}\,d\theta} \quad (4)$$

The FOD density function, *g(θ)*, can also be defined as similar as *g(θ)* with exception that its range varies from 0 to 2π. Hence, the 3D spatial FOD function for composite can be specified for a pair of orientation angles (*θ, ϕ*) as follows [19]:

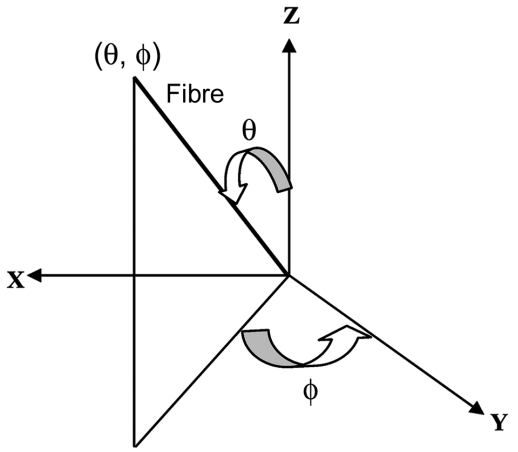

Figure 1. Spatial fibre orientation angles θ and ϕ [18].

$$g(\theta,\phi) = \frac{g(\theta)g(\phi)}{\sin\theta} \quad (5)$$

The previous equation has to comply with two physical conditions: first, the one end of the fibre should be indistinguishable from the other end therefore, the angels turn out to be recurring. Second, every fibre must have a pair of orientation angles, thus the integral of all possible directions or orientation spaces must be equal to unity [19]. The laminate analogy approach (LAA) is used here to evaluate the erosion rate of SFRC. In the LAA, the SFRC can be simulated as a sequence of stacks of various lamina with different fibre orientations. Then, this composite is regarded as a combination of laminates, each comprising fibres having the same *ϕ* (L(ϕ_i), *i=1, 2,..., n*" denotes the *i th* laminate containing fibres of the same *ϕ*).

Each laminate with the same fibre angle is then treated as a stacked sequence of laminae; each lamina consists of fibres having the same ϕ and the same fibre orientation, (L(ϕ_i,θ_j), *j=1, 2,…, m*" denotes the *jth* lamina containing fibres having the same ϕ_i and the same angle *θ*). To calculate the erosion rate of the SFRC in the "Z" direction (Figure 1) using the LAA assumption, it is required initially to evaluate the thermal conductivity of the corresponding unidirectional composite assuming all the fibres lie in the Y-Z plane. Calculation of unidirectional composite erosion rate is explained in the next section.

Composite Erosion Rate

Ambrosio et al. [23] have developed a model of

$$D_{me} = D_m(T_w, p) = \frac{1}{\rho_m}\left(\frac{J_m^0 k_m}{c_m}\right)^{1/2}\left(\frac{6p}{\sigma_{mT}}\right)^{\omega}\left(\frac{RT_w}{E_{am}}\right)^{1/2}\exp\left(-\frac{E_{am}}{2RT_w}\right) \quad (6)$$

$$D_{mi} = D_i = \left(\frac{J_m^0 k_m}{\rho_m c_m}\right)^{1/2}\left(\frac{6\rho_m l_0}{K\sigma_{mT}}\right)^{2\omega-1}\left(\frac{RT_w}{E_{am}}\right)^{\omega}\exp\left(-\frac{E_{am}\omega}{RT_w}\right) \qquad \omega = 5/7 \quad (7)$$

$$p = \rho_g v_g^2 \quad (8)$$

$$D_f(T_w, p) = \frac{1}{\rho_f}\left(\frac{J_f^0 k_f}{c_f}\right)^{1/2}\left(\frac{6p}{\sigma_f}\right)^{\omega}\left(\frac{RT_w}{E_{af}}\right)^{1/2}\exp\left(-\frac{E_{af}}{RT_w}\right) \quad (9)$$

Scheme I.

erosion describing the erosion process as a sequential destruction of the porosity in charring material. Erosion rate of a surface layer of energetic material under the action of pore pressure is known as combustion rate or D_i. The expression for D_i is determined on the basis of joint solution of the heat-conductivity, filtration equations and kinetic equation describing the pyrolysis process in a quasi-static approximation.

The eqns (6) and (7) have been obtained for the thermo-mechanical erosion rate of non-reinforced isotropic materials [16] as shown in Scheme I.

The equation parameters have been totally described in the Symbols section and "p" is the pressure head of the flow at surface that can be defined as eqn (8) in Scheme I.

in eqn (8), ρ_g is the gas density and v_g is the flow velocity. The model is based on the presentation of the pores in the form of hollow cubes with varying wall thickness. While the material is heated, the wall thickness porosity decreases and at a certain time a failure occurs in wall porosity under the action of pressure. The process of thinning of wall pores is caused by matrix pyrolysis. Therefore in eqn (6), the activation energy of thermo-mechanical erosion, E_{am}, corresponds to the activation energy of matrix thermo-decomposition erosion [16].

In order to find the rate of thermo-mechanical erosion of composite, the equation should be divided into two components, erosion rate of matrix and erosion rate of fibres. Although, fibres are not independent constructional material, excluding matrix, theoretically similar equation can be considered as eqn (9) for the fibres as shown in Scheme I, where σ_f is the strength of the monofibres at perpendicular directions and k_f, σ_f, and c_f are thermal conductivity, density and heat capacity of the fibres, respectively.

Short fibre composites have complex geometrical structures. To determine the short fibre composites linear erosion rate, a simplifying assumption has been used with the presumption that all the short fibres in the composite are laid in the same direction. The external thermo-mechanical erosion rate of a unidirectional composite (D'_u) can be determined with the help of the model presented in Figure 2a in the form of a multilayer material consisting of periodically repeated layers of a matrix and hypothetical fibre material:

$$D_u' = \frac{h_m + h_f}{t_m + t_f} \quad (10)$$

$$t_m = h_m / D_m \quad , \quad t_f = h_f / D_f \quad (11)$$

where, h_m and h_f are thicknesses of the layers and t_m and t_f are times during which a complete recession of one layer of the matrix and fibre occurs, respectively [16]. Substituting eqn (11) into eqn (10) yields the final results for the erosion rate of a unidirectional composite as follows:

$$D_u' = \left(\frac{1-\delta_m}{D_f} + \frac{\delta_m}{D_{me}}\right)^{-1} \quad (12)$$

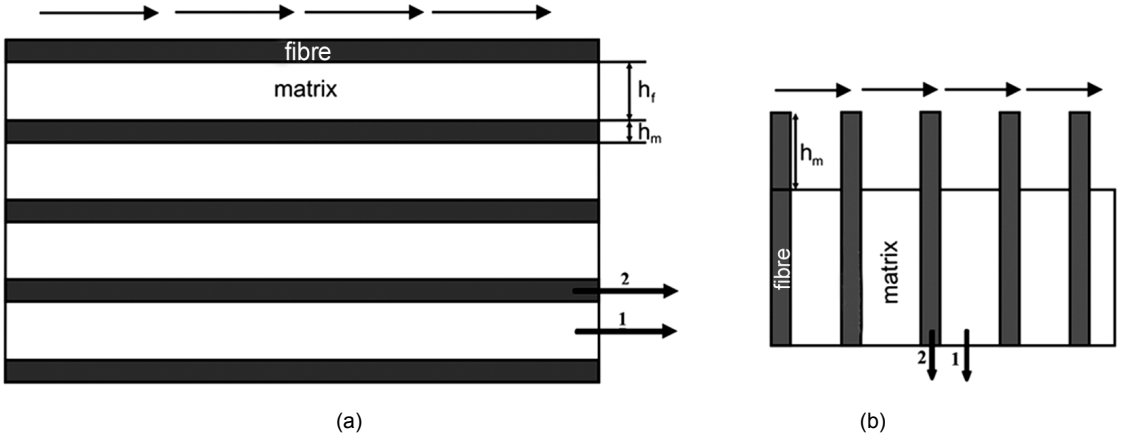

Figure 2. External thermo-mechanical erosion of composite: (a) erosion of unidirectional composite for determination of rate D'_u and (b) erosion of unidirectional composite for determination of rate D_u ((1) matrix and (2) fibre) [16].

where, $\delta_m=h_m/(h_m+h_f)$ would be the relative thickness of interlayer matrix between the layers of fibres in the unidirectional composite.

The erosion rate on the composite surface under the action of a gas flow across the direction of the fibres is defined as D_u. According to Dimitrienko et al. [16] a total rate of recession of the multilayer material, D_u, would be numerically close to the value of recession rate of the fiber:

$$D_u = D_f \tag{13}$$

Eqns (12) and (13) describe the erosion rate of unidirectional composites in longitudinal and transverse directions, respectively.

In the case of a short-fibre unidirectional composite, at time t, there are n fibres that are eroded by the hot gas flow. At $t+\Delta t$, it is assumed that m fibres are completely eroded or torn away from the composite surface. In the same time, some fibres which have reached the composite surface begin to be abraded. A simplifying assumption is that at any time, the number of corroded fibres is constant. With this assumption, eqns (12) and (13) can be used to calculate the erosion rate of the unidirectional short fibre composites.

The above mentioned assumption is depicted in Figure 3. For a thin laminate in which all the fibres lay in the same angle of θ, the erosion rate will be calculated as follows:

$$D_\theta = D_u \sin^2\theta + D'_u \cos^2\theta \tag{14}$$

The erosion rate of a multi laminate short fibre composite with random orientation is then given by:

$$D = \int_{\theta_{min}}^{\theta_{max}} D_\theta g(\theta)\, d\theta \tag{15}$$

By importing eqns (4) and (14) into eqn (15), the resulting equation indicates that the erosion rate of the random short fibre composites depends on materials characteristics, e.g., density, ρ, heat capacity, c, thermal conductivity, k, intensity of volumetric ablation J^0, activation energy, E_a, ultimate strength of matrix and fibre, the surface temperature (T_w) and pressure head of the flow passing over the

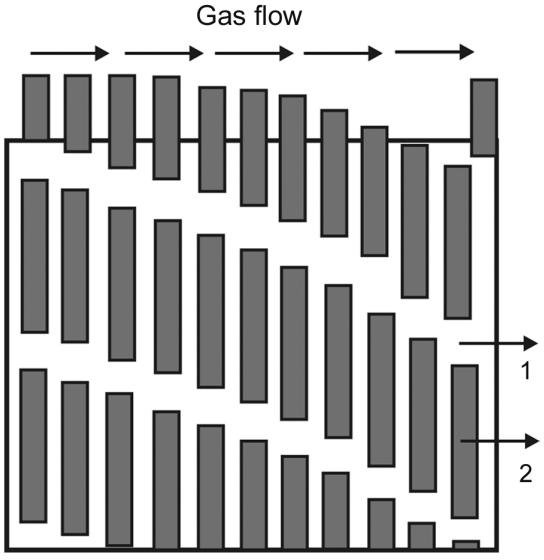

Figure 3. Thermo-mechanical erosion of unidirectional short fibre composite. ((1) matrix and (2) fibre)

material surface. This equation has been achieved by considering two assumptions which describe that the erosion of the unidirectional short fibre composites is equal to long fibre composite and all the fibres may be eroded which means that none of them can be pulled out of the matrix mechanically. Eventually, the final equation has been solved by Matlab Program. The parameters have been separately calculated and the obtained results are discussed later.

EXPERIMENTAL

Materials

Phenolic resin (IL502) was obtained from Resitan Co., Iran, used as a polymeric matrix in composite. The physical properties of the resin are given in Table 1. Short carbon fibres supplied by UVICOM Co. Ltd., Russia were added as reinforcement of the polymeric matrix. The physical properties parameters of the carbon fibres are also given in Table 2.

Sample Preparation

Phenolic resin powder was mixed with ethanol at the predetermined ratio 55/45 for 3 h. Stearic acid as releasing agent was added initially into the mixture. Then, it was mixed with short carbon fibres with a stirrer at 120 rpm for an hour until the carbon fibres were fully impregnated by phenolic resin mixture. The fibre/resin ratio was adjusted to 50/50 wt% (38/62 vol%). Subsequently, the samples were placed in vacuum oven at 80°C for one hour. After degassing, impregnated fibres were placed inside a compression mould under 50 bar pressure and heated to 150°C with the heating rate of 7°C/min to be cured for one hour.

Table 1. Physical properties of phenolic resin.

Characteristics	Unit	Value
Matrix density, ρ_m	$kg.m^{-3}$	1050
Heat capacity, c_m	$J.kg^{-1}.k^{-1}$	2000
Thermal conductivity, k_m	$J.m^{-1}.s^{-1}.k^{-1}$	0.35
Activation energy, E_{am}	$J.mol^{-1}$	98700
Intensity of volumetric ablation, J^0_m	$kg.m^{-3}.s^{-1}$	320000
Ultimate strength of matrix in tension, σ_{mT}	MPa	18

Table 2. Physical properties of carbon fibre.

Specification	Unit	Value
Fibre length	mm	5
Fibre diameter	μm	7
Fibres density, ρ_f	$kg.m^{-3}$	1700
Heat capacity, c_f	$J.kg^{-1}.k^{-1}$	600
Thermal conductivity, k_f	$J.m^{-1}.s^{-1}.k^{-1}$	14
Activation energy, E_{af}	$J.mol^{-1}$	54000
Intensity of volumetric ablation, J^0_f	$kg.m^{-3}.s^{-1}$	550
Ultimate strength of fibres in tension, σ_f	MPa	2200

Test Method

The specific heat and heat of ablation of the carbon/phenolic composite, produced by the above described method, were measured by a Shimadzu DSC-60, Japan, with constant 10 K/min heating rate. Furthermore, the ablation kinetic parameters were obtained by using Shimadzu TGA-50, Japan, with the heating rate of 10 K/min under nitrogen atmosphere. The thermal conductivity coefficient of the composite was measured according to ASTM E1225-87 by means of a Cussons thermal conductivity apparatus, (model P5687, England) and the composite density was obtained in accordance with ASTM D4018. The obtained results are reported in Table 3.

With the purpose of evaluating the ablation performance of the fabricated composites, the oxy-acetylene flame test was carried out according to ASTM E0285-80. During this test hot gases flowed with 3000 K and 8×10^6 $W.m^{-2}$ heat flux was produced. The composite samples prepared for surface erosion measurement have cylindrical shape with 25 mm height and 10 mm diameter. The test results including the ablation surface temperature which was measured by a pyrometer were useful to

Table 3. Physical properties of carbon fibre/phenolic composite.

Characteristics	Unit	Value
Composite density, ρ_c	$kg.m^{-3}$	1297
Heat capacity, c_c	$J.kg^{-1}.k^{-1}$	1300
Thermal conductivity, k_c	$J.m^{-1}.s^{-1}.k^{-1}$	0.901
Char density, ρ_{char}	$kg.m^{-3}$	850

Table 4. Oxyacetylene test condition.

Characteristics	Series 1	Series 2	Series 3
Heat flux ($W.m^{-2}$)	8×10^6	8×10^6	8×10^6
Flame temperature (K)	3000	3000	3000
Pressure head (kPa)	19	30	40
Flow velocity (m/s)	250	300	365
Test time (s)	20	20	20

indicate the ablation and thermal behaviour of the samples. The test method specifies the surface erosion of ablative materials when the samples were exposed to a steady flow of hot gas provided by an oxyacetylene burner.

In order to acquire the back surface temperature, composite sheets of 100×100 mm area and 4 mm thickness were fabricated. Then, an aluminum sheet of 2 mm thickness was located on the rear side of the composite sheets. A hole of 1 mm diameter and 1mm depth for locating the heat sensor was provided on the aluminum sheet. In this way, the thermal insulation effectiveness of the ablative materials can be determined.

In order to compare the theoretical simulation with experimental data, three series of tests were conducted for different values of pressure head and gas flow. In each series three samples prepared under the same conditions were tested. In all tests, the heat flux was set at 8×10^6 $W.m^{-2}$ and hot gas pressure head was changed. At the end of each test, the total erosion, surface temperature and weight loss were measured. The experimental test conditions are listed in Table 4.

RESULTS AND DISCUSSION

To estimate the capability of the model developed, numerical calculations have been conducted for different samples and the results have been compared with the experimental data. Erosion rates and surface temperatures of samples, measured directly by oxyacetylene test for three different pressure heads and flow, are given in Table 5.

The erosion rate, calculated by the model and the experimental data obtained from oxyacetylene test are shown and compared in Figure 4. As can be seen in Figure 4, the experimental data are in good agreement with the calculated values. At lower

Table 5. Erosion rate and surface temperature of samples in oxyacetylene test.

Sample	Sample length (mm)	Erosion rate (mm/s)	Surface temperature (°C)	Weight loss (%)
Series 1[a]				
1	25	0.050	2200	29
2	25	0.045	2230	27
3	25	0.050	2220	28
Series 2[b]				
1	25	0.060	2275	30
2	25	0.058	2290	32
3	25	0.060	2260	31
Series 3[c]				
1	25	0.070	2310	35
2	25	0.065	2320	36
3	25	0.065	2325	35

[(a)] At pressure head 19 kPa and flow velocity 250 m/s; [(b)] at pressure head 30 kPa and flow velocity 300 m/s; [(c)] at pressure head 40 kPa and flow velocity 365 m/s.

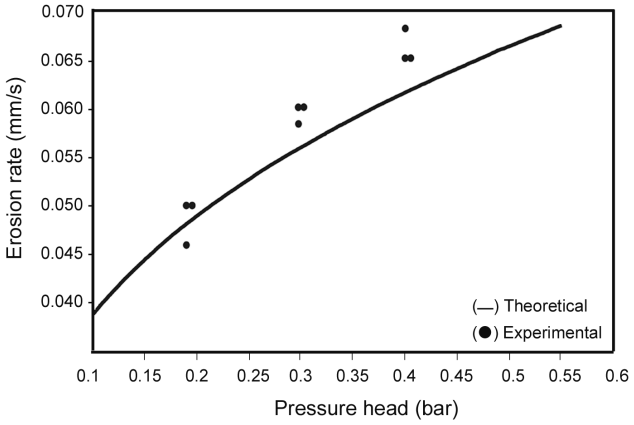

Figure 4. Thermo-mechanical erosion of carbon fibre/ phenolic composite vs. pressure head.

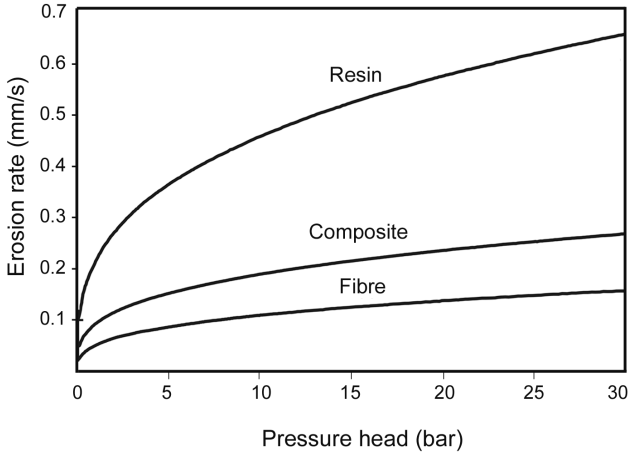

Figure 5. Erosion rate of the composite, resin and carbon fibres vs. pressure head value.

pressure heads, the composite is subjected to lower mechanical stresses, and hence, the fibres are not pulled out of the matrix and are, therefore, eroded gradually. As a result, the theoretical values correlate with the experimental data. The mechanical stresses arise as the pressure head increases. The higher mechanical stresses caused some of the fibres to be pulled out of the matrix before they were being completely eroded. This phenomenon increases the erosion rate of the composite. Since, the fibre-pull out has not been taken into account in the applied computer modelling, at high pressure heads, the predicted values for the erosion rate have deviated from those of the experimental results.

At pressure head of 19 kPa, the theoretical and experimental values of the erosion rates were 0.048 mm/s and 0.05 mm/s, respectively. Twenty seconds after the beginning of the test, the theoretical and experimental values of the surface erosion were 0.96 and 1 mm, respectively. When the pressure head value reached 30 and 40 kPa, the difference between the experimental and theoretical values elevated to 6.67% and 5.4%, correspondingly which are slightly higher than the difference of 4% between these values at the lower pressure head of 19 kPa.

Figure 5 shows the effect of pressure head values on the erosion rate of the composite according to the theoretical modelling which have been derived from above equations. It is apparent that as a result of increasing the pressure head, the erosion rate of the composite goes up. As it is seen, the efficacy of pressure head on the mechanical erosion rate is higher at lower pressure head values and its influence becomes less apparent especially when the pressure head value is higher than 500 kPa (5 bar). In other words, in higher pressure heads the composite erosion rate increases gradually. This observation can be likewise concluded from eqns (6)-(9).

The erosion rates of phenolic resin and carbon fibres versus pressure head values are also depicted in Figure 5. The mechanical erosion of the matrix is considerably higher than that of the fibre due to lower tensile strength of the matrix in comparison with the tensile strength of the fibre. In Figure 5, it can be seen that phenolic matrix is eroded more rapidly than the carbon fibre/phenolic composite which signifies the higher resistance of the latter composite against erosion as compared with its constituents. In addition, the composite surface temperature affects the erosion rate of its components dramatically.

Figure 6 presents the influence of the surface temperature on the erosion rate of the composite at different values of the pressure head. It is clear that as a consequence of surface temperature rising as well as pressure head increment, the erosion rate accelerates remarkably. This is attributed to the more apparent erosion rate of the matrix with respect to surface temperature that increases the erosion rate of the composite.

Back surface temperature can also be measured during the oxyacetylene test according to the method described previously. Figure 7 indicates the back

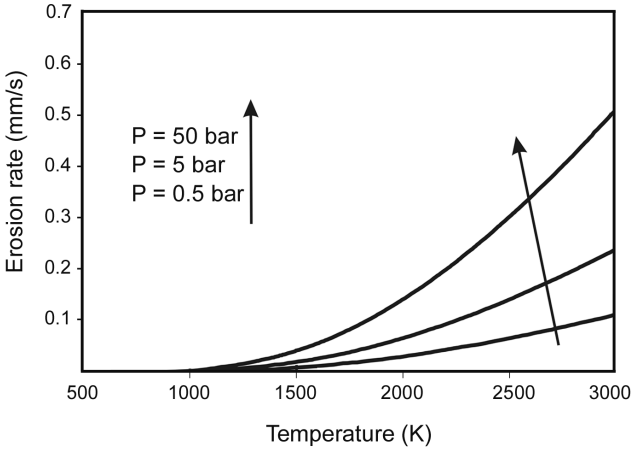

Figure 6. Erosion rate of the composite vs. the surface temperature at different pressure head values.

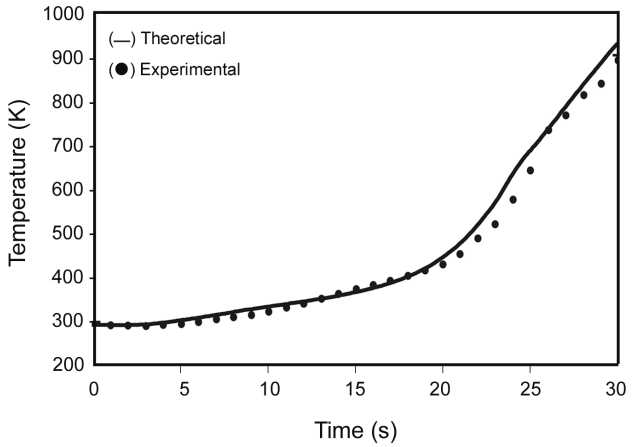

Figure 7. Prediction of back surface temperature in oxyacetylene test.

surface temperatures of carbon/phenolic composite versus experiment time which have been calculated according to the model derived by Bahramian et al. [1].

The kinetic parameters such as frequency factor and degree of thermal degradation reaction that have been determined by employing TGA results are reported in Table 6 and used to calculate the back surface temperatures of the composite sheets.

Experimental data that are obtained by oxyacetylene flame tests are reported in Figure 7, as well. The test time duration is 30 s and the front surface temperature rises up to 2325 K. In the oxyacetylene test, the experimental back surface temperature increases up to 888.6 K during 30 s. A similar trend has been observed for results obtained by the theoretical model in which the temperature has been raised to 930.7 K by equal time intervals. As can be seen, the results have a good correlation at the first 18 s and after that, partial deviation is observed. Initially the erosion rate is very low and that is because the degradation process has not started at the depth of the samples.

As the test time prolongs the back surface

Table 6. Thermal degradation kinetic parameters of composite.

Property	Symbol	Unit	Value
Frequency factor	A	s^{-1}	8.14×10^{4}
Degree of thermal degradation reaction	n	-	3.2
Heat of ablation	H	J/kg	3.134×10^{5}
Composite thermal conductivity	k_c	J/m.s.k	0.901
Specific heat of composite	c_p	J/kg.k	1300
Density of composite	ρ	kg/m^3	1297
Primary temperature	T_0	K	292
Surface temperature	Tw	K	2470
Air heat transfer coefficient	h	$J/m^2.s.K$	10
Specific heat of flowing gas	c_g	J/kg.K	1680
Molecular weight of outlet gas	M_{wg}	kg/mol	16
Gasification coefficient of the matrix	Γ	-	0.6
Gas global constant	R	J/mol.K	8.314
Thickness of Samples	y	m	4.1×10^{-3}

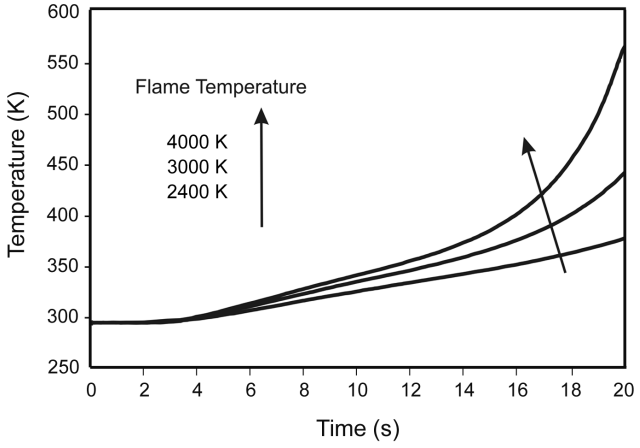

Figure 8. Effect of flame temperature on back surface temperature.

temperature begins to increase noticeably which is due to the continuous erosion of the ablative materials that increases the heat transfer mechanism. It is observed that after 19 s, the predicted temperatures are higher than the actual ones which have actually originated from the difference between the rate of the theoretical and actual erosions.

Figure 8 shows the effect of flame temperature on the back surface temperature. It is evident that by decreasing the flame temperature from 3000 K to 2400 K, the back surface temperature decreases from 428 K to 364 K in 20 s which confirms the direct effect of flame temperature on the back surface temperature. The influence of two different composite erosion rates (i.e., 2.5 and 5 mm.s^{-1}) on the back surface temperature is indicated in Figure 9.

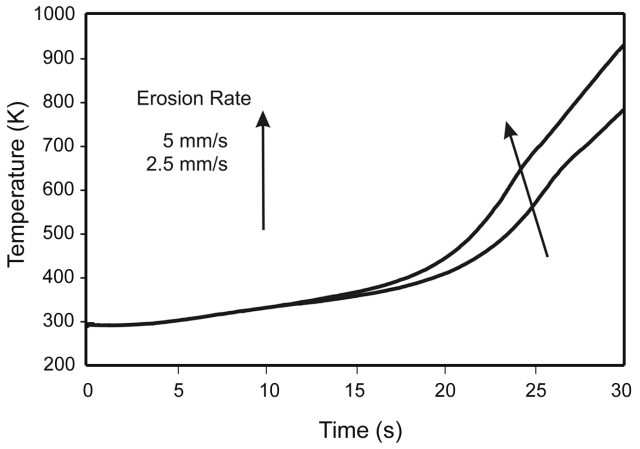

Figure 9. Effect of erosion rate on back surface temperature.

When the erosion rate doubles, the back surface temperature increases from 780 K to 930 K after 30 s.

CONCLUSION

A mathematical model is developed to predict the erosion rate of short carbon fibre phenolic composites exposed to a hot gas flow. The model not only considers the thermo-chemical process but also takes into account the thermo-mechanical erosion of the composite. The comparison of the experimental data with those calculated by the model indicates good correlation at 19 kPa (0.19 bar) pressure head. At higher pressure rates, however, there is a slight deviation between the experimental and calculated results. The deviation is attributed to the fibre-pull out mechanism that causes the removal of the fibres prior to their absolute erosion as the pressure head increases. The model also indicates that the erosion increases rapidly when the surface temperature of the composite rises above 1000 K. Furthermore, the model is able to predict the erosion of the composite as a function of the applied pressure head and the temperature at the surface of the composite. Eventually, the effect of the flame temperature and erosion rate on elevation of back temperature has been clarified by the model. In general, the developed model has been adequately approved by the experimental data of ablation behaviour of the carbon fibre/phenolic composite.

SYMBOLES

c_m : Heat capacity of matrix (J.kg^{-1}.K^{-1})
c_f : Heat capacity of fibres (J.kg^{-1}.K^{-1})
D_m : Erosion rate of matrix (m.s^{-1})
D_f : Erosion rate of fibres (m.s^{-1})
D_u : Erosion rate of unidirectional composite in transverse directions (m.s^{-1})
D'_u : Erosion rate of unidirectional composite in transverse directions (m.s^{-1})
D_θ : Erosion rate of a thin laminate in which all the fibres lied under the same angle θ (m.s^{-1})
E_{am} : Activation energy of matrix (J.kg^{-1})

E_{af} : Activation energy of fibres (J.kg^{-1})
$g(\theta)$: Fibres orientation distribution function
h_m : Thicknesses of the matrix layer (m)
h_f : Thicknesses of the fibres layer (m)
J^0_m : Intensity of the volumetric ablation of matrix (kg.m^{-3}.s^{-1})
J^0_f : Intensity of the volumetric ablation of fibres (kg.m^{-3} s^{-1})
k_m : Thermal conductivity of matrix (J.m^{-1}.s^{-1}.K^{-1})
k_f : Thermal conductivity of fibres (J.m^{-1}.s^{-1}.K^{-1})
k_c : Thermal conductivity of composite (J.m^{-1}.s^{-1}.K^{-1})
p : Pressure head (Pa)
r : Shape parameters
R : Universal gas constant (J.mol^{-1}.K^{-1})
q : Shape parameters
T_w : Surface temperature (K)
t_m : Times during which a complete recession of one layer of matrix occurs
t_f : Times during which a complete recession of one layer of fibres occurs
l_0 : Characteristic diameter of pores
ρ_m, : Matrix density (kg.m^{-3})
ρ_f, : Fibres density (kg.m^{-3})
ρ_g, : Gas density (kg.m^{-3})
ρ_{char} : Char density (kg.m^{-3})
σ_{mT}, : Ultimate strength of matrix in tension (Pa)
σ_f : Ultimate strength of fibres in tension (Pa)
v_g : Flow velocity (m.s^{-1})
δ_m : Relative thickness of matrix
θ , ϕ : Spatial fibre orientation angles

REFERENCES

1. Bahramian AR, Kokabi M, Famili MHN, Beheshti MH, Ablation and thermal degradation behavior of a composite based on resol type phenolic resin: process modeling and experimental, *Polymer*, **47**, 3661-3673, 2006.
2. Bahramian AR, Kokabi M, Beheshti MH, Famili MHN, Thermal degradation process of resol type phenolic matrix/kaolinite layered silicate nanocomposite, *Iran Polym J*, **16**, 375-387, 2007.
3. Lee YJ, Joo HJ, Ablation characteristics of carbon fiber reinforced carbon (CFRC) composites in the presence of silicon carbide (SiC) coating, *Surface Coat Technol*, **180-181**, 286-289, 2004.
4. Ren F, Sun HS, Liu LY, Theoretical analysis for mechanical erosion of carbon-base materials in ablation, *J Thermophys Heat Tr*, **10**, 593-597, 1996.
5. Fu SY, Mai YW, Lauke B, Yue C-Y, Synergistic effect on the fracture toughness of hybrid short glass fiber and short carbon fiber reinforced polypropylene composites, *Mat Sci Eng A-Struct*, **323**, 326-335, 2002.
6. Fu S-Y, Lauke B, Mader E, Yue C-Y, Hu X, Mai Y-W, Hybrid effects on tensile properties of hybrid short-glass-fiber-and short-carbon-fiber-reinforced polypropylene composites, *J Mater Sci*, **36**, 1243-1251, 2001.
7. Sarasua JR, Remiro PM, Pouyet J, The mechanical behavior of PEEK short fiber composites, *J Mater Sci*, **30**, 3501-3508, 1995.
8. Shiao ML, Nair SV, Garrett PD, Pollard RE, Effect of glass-fiber reinforcement and annealing on microstructure and mechanical behavior of nylon 6,6, *J Mater Sci*, **29**, 1973-1981, 1994.
9. Zhou J, Li G, Li B, Tinabai H, Flexural fatigue behavior of injection-molded composites based on poly(phenylene ether ketone), *J Appl Polym Sci*, **65**, 1857-1864, 1997.
10. Ranganathan S, Advani SG, Characterization of orientation clustering in short-fiber composites, *J Polym Sci Polyn Phys*, **28**, 2651-2672, 1990.
11. Biolzi L, Castellani L, Pitacco I, On the mechanical response of short fiber reinforced polymer composites, *J Mater Sci*, **29**, 2507-2512, 1994.
12. Fu S-Y, Lauke B, Mader E, Yue C-Y, Hu X, Tensile properties of short-glass-fiber- and short-carbon-fiber-reinforced polypropylene composites, *Compos Part A-Appl S*, **31**, 1117-1125, 2000.
13. Fu S-Y, Mai Y-W, Thermal conductivity of misaligned short-fiber-reinforced polymer composites, *J Appl Polym Sci*, **88**, 1497-1505, 2003.
14. Shen H, Nutt S, Hull D, Direct observation and measurement of fiber architecture in short fiber- polymer composite foam through micro-CT imaging, *Compos Sci Technol*, **64**, 2113-2120, 2004.
15. Singh R, Chen F, Jones R, Injection molding of glass fiber reinforced phenolic compos. 2: study of

the injection molding process, *Polym Compos*, **19**, 37-47, 1998.
16. Dimitrienko YI, Dimitrienko ID, Effect of thermomechanical erosion on heterogeneous combustion of composite materials in high-speed flows, *Combust Flame*, **122**, 211-226, 2000.
17. Kumar S, Satapathy BK, Patnaik A, Thermo-mechanical correlations to erosion performance of short carbon fibre reinforced vinyl ester resin composites, *Mater Design*, **32**, 2260-2268, 2011.
18. Vignoles GL, Aspa Y, Quintard M, Modeling of carbon-carbon composite ablation in rocket nozzles, *Compos Sci Technol*, **70**, 1303-1311, 2010.
19. Fu S-Y, Lauke B, An analytical characterization of the anisotropy of the elastic modulus of misaligned short-fiber-reinforced polymers, *Compos Sci Technol*, **58**, 1961-1972, 1998.
20. Lauke B, Fu S-Y, Strength anisotropy of misaligned short-fiber-reinforced polymers, *Compos Sci Technol*, **59**, 699-708, 1999.
21. Fu S-Y, Lauke B, The elastic modulus of misaligned short-fiber-reinforced polymers, *Compos Sci Technol*, **58**, 389-400, 1998.
22. Fu S-Y, Lauke B, Effects of fiber length and fiber orientation distributions on the tensile strength of short-fiber-reinforced polymers, *Compos Sci Technol*, **56**, 1179-1190, 1996.
23. Ambrosio G, Tritto I, Golino P, Dimitrienko YI, Modeling of erosion combustion of energetic materials in high-enthalpy flows, *Combust Flame*, **111**, 161-174, 1997.